

# A new conceptual model on the fate and controls of fresh and pyrolyzed plant litter decomposition

Jennifer L. Soong · William J Parton ·  
Francisco Calderon · Eleanor E. Campbell ·  
M. Francesca Cotrufo

Received: 6 May 2014 / Accepted: 12 February 2015 / Published online: 25 February 2015  
© Springer International Publishing Switzerland 2015

**Abstract** In recent years, litter decomposition studies have begun to move beyond the concept of mass loss to consider the fate of fresh and pyrolyzed decomposing plant material in the ecosystem. However, these concepts have yet to be incorporated into conceptual models of litter decomposition. Understanding how fresh and pyrolyzed plant litter chemical traits control the partitioning of mass loss to dissolved organic carbon (DOC) leaching and respiration to CO<sub>2</sub> would help to inform models of litter-soil-atmosphere carbon (C) cycling. To test these controls, we incubated five fresh and one pyrolyzed leaf litters with differing chemistry and measured DOC and CO<sub>2</sub> fluxes as well as changes in substrate and dissolved organic matter (DOM) chemistry over time using Fourier transformed infrared spectroscopy and wet chemistry. We found that the amount of hot water

extractable C was a strong predictor of initial DOC leaching, while the lignocellulose index [Lignin/(Lignin +  $\alpha$ -Cellulose)] was a strong inverse predictor of later stage DOC:CO<sub>2</sub> partitioning. Changes in substrate and DOM chemistry indicated a progression of substrate availability for leaching: from soluble plant components, to partially decomposed cellulose and lignin, to microbial products. Based on these results we developed a new conceptual model that demonstrates how chemical traits of fresh and pyrolyzed plant litter can be used to predict the fate of aboveground organic matter decomposition and form a better linkage between aboveground decomposition and terrestrial ecosystem C cycling.

**Keywords** Leaf litter · Pyrogenic organic matter · Decomposition · Dissolved organic matter · Dissolved organic carbon · Leaching · Respiration · FTIR

---

Responsible Editor: Asmeret Asefaw Berhe.

---

J. L. Soong (✉) · W. J Parton · E. E. Campbell ·  
M. F. Cotrufo  
Natural Resource Ecology Laboratory, Colorado State  
University, Fort Collins, USA  
e-mail: Jennifer.soong@colostate.edu

F. Calderon  
Central Great Plains Research Station, USDA-ARS,  
Akron, USA

M. F. Cotrufo  
Department of Soil and Crop Sciences, Colorado State  
University, Fort Collins, USA

## Introduction

Aboveground plant litter decomposition is a key component of carbon (C) and nutrients cycling in terrestrial ecosystems, generating products such as CO<sub>2</sub> and microbially processed or partially decomposed organic matter (OM) that connects aboveground plant production to both the atmosphere and soils. Traditionally, studies of litter decomposition have focused on measurements of litter mass loss rates using litter bags (Bocock and Gilbert 1957), or on CO<sub>2</sub>

production in laboratory incubations (e.g., Couëteux et al. 1991; Li et al. 2011), assuming that litter C lost during decomposition is oxidized to CO<sub>2</sub> (Cotrufo et al. 2009). Within this framework, litter mass is generally lost until it reaches a non-zero asymptote, with the remaining indecomposable solid mass providing the main litter C contribution to soil organic matter (SOM) formation (Berg and McLaugherty 2003; Chapin et al. 2002). These classic models focus on mass loss rates, and interpret chemical changes in the mass remaining as resulting from selective preservation of individual plant litter components (Berg and McLaugherty 2003), as well as the formation of secondary product by microbial decomposers (Chapin et al. 2002). However, they do not consider the fate of the litter mass that is lost, nor do they capture the potential for interactive controls between different plant litter components over time. A new conceptual framework describing the relationship between plant litter traits, dissolved organic matter (DOM), and CO<sub>2</sub> production during fresh and pyrolyzed plant litter decomposition will help to link litter decomposition to soil and ecosystem C cycling.

New evidence suggests that 6–39 % of C loss during leaf litter decay enters the soil in the form of dissolved organic C (DOC) during the early phases of decomposition (Qualls and Haines 1991; Magill and Aber 2000; Don and Kalbitz 2005), and plays a significant role in SOM formation and long-term soil C sequestration (Kaiser and Kalbitz 2012; Cotrufo et al. 2013). The ability to estimate the partitioning of litter mass loss between DOC:CO<sub>2</sub> during decomposition would greatly improve our ability to predict aboveground litter contributions to SOM formation across different ecosystems and under future global change scenarios. What controls this partitioning? Beside climate, litter chemistry is the main controlling factor of litter mass loss rates (Aber et al. 1990; Li et al. 2011) and CO<sub>2</sub> efflux from litter decomposition (Hessen et al. 2004). In particular, lignin and nitrogen (N) content (Melillo et al. 1982; Berg and Matzner 1997), as well as the Lignocellulose index (LCI) [lignin/(lignin +  $\alpha$ -cellulose)] (Osono and Takeda 2005), have been shown to be good predictors of litter mass loss rates and carbon use efficiency (CUE) (Manzoni et al. 2012; Moorhead et al. 2013).

Plant litter can broadly be categorized into a soluble fraction, cellulose and hemicellulose (otherwise referred to as carbohydrates), and lignin, as in the classic

models presented by Berg and McLaugherty (2003) and Chapin et al. (2002), with secondary compounds being produced by microbes over time and accumulating in the litter residue. Although lignin is known to control litter mass loss rates, it is still not fully understood whether lignin is selectively preserved (Berg and McLaugherty 2003), continuously degraded (Preston et al. 2009b) or preferentially degraded (Klotzbucher et al. 2011) during the decomposition process, nor how it may interact with other litter components to control mass losses to DOC:CO<sub>2</sub> (Kalbitz et al. 2006; Klotzbucher et al. 2011). Beyond lignin, other chemical characteristics of plant residues such as their lignin-to-N ratio (Adair et al. 2008) or functional group biochemistry (Gallo et al. 2005) may affect C dynamics during decomposition.

Fourier transformed mid-infrared (FTIR) spectroscopy can be used to identify the functional group chemistry of fresh or pyrolyzed plant material and DOM, and thus provide a sensitive and inexpensive method for analyzing the chemical changes of litter and DOM over the course of decomposition (Lammers et al. 2009; Strobel et al. 2001; Gallo et al. 2005; Soong et al. 2014). FTIR has been used to detect several absorbance bands in litter extracts including: 3400 cm<sup>-1</sup> for O–H or N–H, 2850–2930 cm<sup>-1</sup> for aliphatic C–H, 1605 cm<sup>-1</sup> for aromatic C=C, and at 1070 cm<sup>-1</sup> for polysaccharides (He et al. 2009). FTIR analysis of forest floor litter, litter fiber and lignin fractions showed the following informative bands: carbonyl absorption bands at 1724 cm<sup>-1</sup> (esters) and 1659 cm<sup>-1</sup> (proteins), as well as the 1603 cm<sup>-1</sup> band assigned to lignin from aromatic skeletal vibrations (Galletti et al. 1993). Thus, FTIR functional group chemistry can be used to study differences in plant input chemistry between species and in litter residues over the course of decomposition.

If litter chemistry controls not only mass loss rates, but also the partitioning of C losses between CO<sub>2</sub> and DOC leaching to the soil, we can expect large changes in litter-soil C fluxes to occur as a consequence of global changes, for example as plant species ranges shift with climate and land use change (Thomas 2010; Kelly and Goulden 2008). The projected increases in the frequency and severity of fire (Stocks et al. 1998; Flannigan et al. 2000) will also change the chemical composition of the plant litter inputs to the soil surface, with larger inputs in the form of pyrogenic organic matter (py-OM). Py-OM is partially combusted plant

material, and is generally considered a chemically recalcitrant substance (Knicker 2011) with estimated overall turnover times on a centennial scale (Singh et al. 2012). However, py-OM has a measureable soluble component that can leach into the soil (Novak et al. 2009) and is partially mineralizable (Stewart et al. 2013; Santos et al. 2012). DOM leaching from fresh litters and py-OM may therefore both be controlled by similar chemistry changes as decomposition progresses.

The objective of this study was to develop a new conceptual model on the relationship between chemical traits and DOC:CO<sub>2</sub> partitioning during the decomposition of fresh and pyrolyzed plant litter based on: (1) the identification of chemical traits that can be used to predict how much mass is lost as leached DOC and respired CO<sub>2</sub> during decomposition, and (2) evidence from changes in the chemical composition of litter and DOM leachate over the course of decomposition. The study we conducted in order to build the conceptual model was designed to specifically test two hypotheses. (H1) DOM leaching represents a significant fraction of mass loss, which is not directly proportional to CO<sub>2</sub> production but rather is controlled by litter chemistry. We hypothesize that plant litters with a large fraction of structural components (e.g., cellulose and lignin) decompose more slowly due to the low CUE of their breakdown (Moorhead et al. 2013), and thus lose more C as CO<sub>2</sub>, while litters with a large fraction of soluble, non-structural, components decompose quickly and lose more C as DOC due to a higher proportion of water soluble compounds. (H2) DOM chemical composition changes over the course of decomposition, reflecting the interactive and sequential leaching of different soluble plant and microbial products as decomposition progresses. We hypothesize that initial DOM leaching reflects the soluble material of the substrates, and then shifts toward partially broken down cellulosic and structural materials and microbial products. Our conceptual model summarizes significant advancements in the field of litter decomposition moving from studies focused solely on decay rates and chemical composition of the remaining litter residue toward those concerned also with the fate and chemical composition of the matter being degraded or lost.

To test the above hypotheses we incubated six substrates, one py-OM and five leaf litters that varied in initial chemistry, and measured DOC and CO<sub>2</sub>

losses during their decomposition. We characterized substrate chemistry based on C:N, % structural material as % cellulose and % acid unhydrolyzable residue (AUR), % non-structural material [total mass-neutral detergent fiber (NDF) mass], % hot water extractable C (HWE-C) and FTIR spectroscopy. We characterized DOM throughout the incubation based on DOC, total dissolved nitrogen (TDN), NH<sub>4</sub><sup>+</sup>, NO<sub>3</sub><sup>-</sup> and FTIR spectroscopy.

## Methods

### Fresh and pyrolyzed litter samples

For this study we used six substrates: five above ground leaf litters and one py-OM sample. We collected ash (*Fraxinus excelsior*), big bluestem (*Andropogon gerardii*), oak (*Quercus macrocarpa*) and pine (*Pinus ponderosa*) leaf litter in the fall of 2011 as freshly senesced litter that had neither hit the ground nor been rained on since abscission. Alfalfa (*Medicago sativa*) leaves were collected standing green at crop maturity. Plant types were selected to cover a range of chemical characteristics such as C-to-N ratio (C:N) and LCI. Abscised ash leaves and pine needles were collected from separate raised litter traps. Senesced oak leaves were shaken off of a tree and collected in a litter trap. Senesced, standing big bluestem grass blades were hand cut from a native tallgrass prairie. We removed all stems and petioles from the leaves, and pooled them each by species. We air dried all litter samples, cut them into 1 × 1 cm pieces or 1 cm lengths, and homogenized them. We did not cut the alfalfa litter, whose leaves were already approximately 1 × 1 cm. To produce a py-OM sample, we placed ground big bluestem grass litter into porcelain crucibles, which were heated at 300 °C for 4 h in a muffle furnace with ultra-high purity nitrogen flow as described by Rutherford et al. (2012). Three subsamples from each litter and py-OM pool were oven dried at 105 °C for dry weight correction, ground, and used for elemental and chemical analysis as described below.

### Laboratory incubation

Three replicates of each substrate, i.e. all five litter types and the py-OM, were incubated for 1 year

(365 days) under optimal laboratory conditions. We incubated an additional set of three replicates per each substrate for 95 days, for destruction at an intermediate time point. For each sample, 2 g of litter or py-OM was placed in leaching cups, 3 cm in diameter (CellSmart Vacuum Filtration Systems, Argos Technologies) fitted on the bottom with a 20  $\mu\text{m}$  nylon filter. Initially, we leached the samples with deionized water on day 0, and then inoculated them with 1 ml of microbial inoculum. We created the inoculum by mixing 1 g of a partially decomposed mixture of grass and deciduous tree litter, collected from a nearby creek bank, with 100 ml deionized water for 2 h. The mixture was left to settle, filtered over a 20  $\mu\text{m}$  nylon filter, and then 1 ml of the filtrate inoculum was added to each sample. We had three blank samples consisting of a leaching cup that was inoculated, with which we quantified any potential microbial degradation of the plastics in the leaching cup, and subtracted this from all DOC and TDN results. Each leaching cup was sealed in an airtight 3.8 l jar fitted with a rubber septum for gas sampling throughout the entirety of the incubation. The jars were periodically checked to ensure air tightness. A thin layer of water at the bottom of the jars maintained constant humidity, and the jars were incubated at a constant temperature of 25 °C in the dark.

We measured  $\text{CO}_2$  and DOM leaching periodically throughout the incubation. We used a gas tight syringe to sample air in the headspace of the jars through the septum, and analyzed it on an infrared gas analyzer (IRGA, Li-Cor 800, Li-Cor, NE) for  $\text{CO}_2$  concentration (Stewart et al. 2013). After  $\text{CO}_2$  collection, we opened the jars and placed the leaching cups on a 250 ml flask for leachate collection. We dispensed 30 ml of deionized water evenly over the litter samples and allowed the leachate to drain through the leaching cup filter and into the collection flask. After 20 min of leaching, we used a light vacuum line to drain out any remaining leachate from the cups. We subsampled the leachate for FTIR analysis as described below, then immediately froze them until further analysis.

After leachate collection, we placed each leaching cup back in the airtight jars and flushed them with soda lime scrubbed air to minimize initial  $\text{CO}_2$  concentrations. We measured this initial  $\text{CO}_2$  concentration to accurately quantify the amount of  $\text{CO}_2$  produced during each incubation period. Jars were then returned

to the constant temperature room until the following sampling. We wanted to prevent  $\text{CO}_2$  from building up to toxic levels in the jars ( $>2\%$ ), so sampling frequency was determined by the maximum rate of  $\text{CO}_2$  production, with more frequent initial sampling tapering off through the duration of the experiment.

### Chemical analysis

We characterized three replicates of initial (day 0), day 95 and day 365 substrate chemistry based on mass remaining, % C, % N, % acid-unhydrolyzable residue (AUR), % acid soluble fiber ( $\alpha$ -cellulose), % neutral-detergent fiber (NDF) and their FTIR spectral properties. For some of the day 365 substrates, not enough mass remained for replicate analysis so the remaining substrate mass was aggregated and analyzed as one replicate sample. All samples were analyzed for % C and % N on an elemental analyzer (LECO tru-SPEC, Leco Corp., St. Joseph, MI). Percent cellulose and AUR were determined using the acid detergent fiber (ADF) digestion method (Van Soest and Wine 1968). In brief, an initial heated digestion in Cetyl trimethylammonium bromide (CTAB) and sulfuric acid removes hemicellulose and other non-structural carbohydrates and lipids, and then the samples are digested in 73 % sulfuric acid. The fiber from this 73 % sulfuric acid digestion will be referred to as cellulose, as it is a proximate estimate of  $\alpha$ -cellulose content, while AUR is a proximate estimate of lignin content (Rowland and Roberts 1994), with both fractions corrected for ash content. Using this proximate analysis, day 0 LCI is calculated as  $[\text{AUR}/(\text{AUR} + \alpha\text{-cellulose})]$ . Additionally, we characterized the initial % non-structural material on three replicates of the day 0 samples using a neutral detergent fiber (NDF) digestion (Van Soest et al. 1991). We also characterized the initial substrates based on HWE-C on three replicates of the day 0 samples, following Tappi (1981). All three replicate samples of the dried, ground samples from day 0, 95 and 365 were also scanned using a Digilab FTS 7000 spectrometer (Varian, Inc., Palo Alto, CA) with a Pike AutoDIFF sampler (Pike Technologies, Madison, WI) for FTIR spectral analysis. The spectrometer had a deuterated, Peltier-cooled, triglycine sulfate detector and potassium bromide (KBr) beam splitter. KBr was used as background. Data were obtained as pseudo-absorbance  $[\log (1/\text{Reflectance})]$ . Each spectrum was

collected at  $4\text{ cm}^{-1}$  resolution, with 64 co-added scans from 4000 to  $400\text{ cm}^{-1}$ .

All leachate samples were thawed and analyzed for total organic carbon (TOC) and TDN on a TOC analyzer (Shimadzu TOC 5000). Inorganic  $\text{NH}_4^+$  and  $\text{NO}_3^-$  of the leachate were measured on days 0, 1, 4, 7, 10, 15, 20, 28, 39, 64, 76, 95, and 284 using an Alpkem Flow Solution IV Automated wet chemistry system (O.I. Analytical, College Station, TX). We also analyzed the leachate chemistry on days 0, 1, 4, 7, 10, 95, 118, 228 and 365 by FTIR analysis. An aliquot (0.5 ml) of leachate was added to 250  $\mu\text{g}$  of KBr and freeze-dried. The dried KBr-leachate samples were scanned using the same spectrometer and settings as the litters.

### Data analysis

We tested the effect of substrate type and incubation time on mass loss, changes in C:N ratio, %  $\alpha$ -cellulose and % AUR by means of a generalized linear mixed model. We included substrate type, time and their interaction as categorical fixed effects. The effects of substrate chemistry on  $\text{CO}_2$  efflux, DOC leaching and the DOC: $\text{CO}_2$  ratio over time was tested by means of a repeated measures test within a generalized linear mixed model containing incubation day, with substrate type and their interaction as categorical fixed effects. Individual samples were treated as random effects within each substrate type. These analyses were carried out using the SAS<sup>®</sup> software version 9.3. The data passed our tests for normality and homogeneity of variances of the residuals. In all cases we used type III tests of fixed effects.

The FTIR spectra from duplicate scans of the time 0 substrates were averaged using GRAMS version 9.1 software with the GRAMS IQ package (Thermo Fisher, Woburn, MA). All spectra were mean-centered before statistical analysis. We utilized a distance-based redundancy analysis (dbrDA) for statistical assessment of the overall differences in FTIR spectral chemistry among substrates and leachate composition over time using the R: Vegan package (Oksanen et al. 2013). Briefly, we chose the dbrDA analysis over other multivariate statistical approaches due to its non-linear distance-metric options, which have robust multi-dimensional resolution to assess categorical variables. Distance based RDA is a three step ordination technique that tests the effects of response

parameters (i.e. absorbance intensity in  $\text{cm}^{-1}$ ) on defined groups (i.e. litter or leachate type at a given incubation time). First, a dissimilarity or distance matrix is calculated for the different litter/leachate types. We chose the Bray–Curtis dissimilarity (non-linear) measure to model the species matrix as suggested by Legendre and Anderson (1999). For steps two and three of the dbrDA, a principal coordinate analysis (PCoA) was calculated based on the distance matrix, from which the eigenvalues (obtained in the PCoA) were applied to a redundancy analysis (RDA). Principal components analysis (PCA) of the spectral data and spectral subtractions were carried out using GRAMS/AI Ver. 9.1 (Thermo Fisher Scientific Inc.). The default autoscale, optimal factor, and tolerance values calculated by the software were used for the subtractions. The spectral data was mean centered before the PCA analysis.

## Results

### Mass loss, DOC and $\text{CO}_2$ dynamics

At the two destructive harvests on day 95 and 365, alfalfa had lost 77 and 83 % of its initial mass respectively; ash 44 and 62 %, oak 45 and 58 %, bluestem 21 and 46 % and pine 18 and 28 % (Table 1). The py-OM lost 4 % of its mass by the end of the incubation and DOC and  $\text{CO}_2$  fluxes were detected, however due to high variance this change in mass was not statistically significant (Fig. 1,  $p > 0.05$ ). We used our measured DOC and  $\text{CO}_2$  values to calculate cumulative DOC and  $\text{CO}_2$ -C losses, relative to the initial litter C basis. At the end of the 365 day incubation, 15 % of the initial C from alfalfa was lost as DOC, 16 % for ash, 10 % for bluestem, 8 % for oak, 3 % for pine, and 1.57 % for the py-OM. For alfalfa, 37 % of the initial C was lost as  $\text{CO}_2$ , 25 % for ash, 18 % for bluestem, 35 % for oak, 15 % for pine, and 2.59 % for py-OM (Table 1).

We also tracked the dynamics of substrate C loss to DOC and  $\text{CO}_2$  over the course of the incubation (Fig. 1). By the end of the experiment the total DOC: $\text{CO}_2$  ratios ranged between 0.20 and 0.65 (Fig. 1). As expected, most of the DOC and  $\text{CO}_2$  fluxes occurred during the initial period of the incubation, with alfalfa decomposing much more rapidly than the other litter types. Ash and bluestem

**Table 1** Average values of litter chemistry at three experimental time points (n = 3 except for day 95 DOC and TDN, where n = 6), standard error is in parentheses

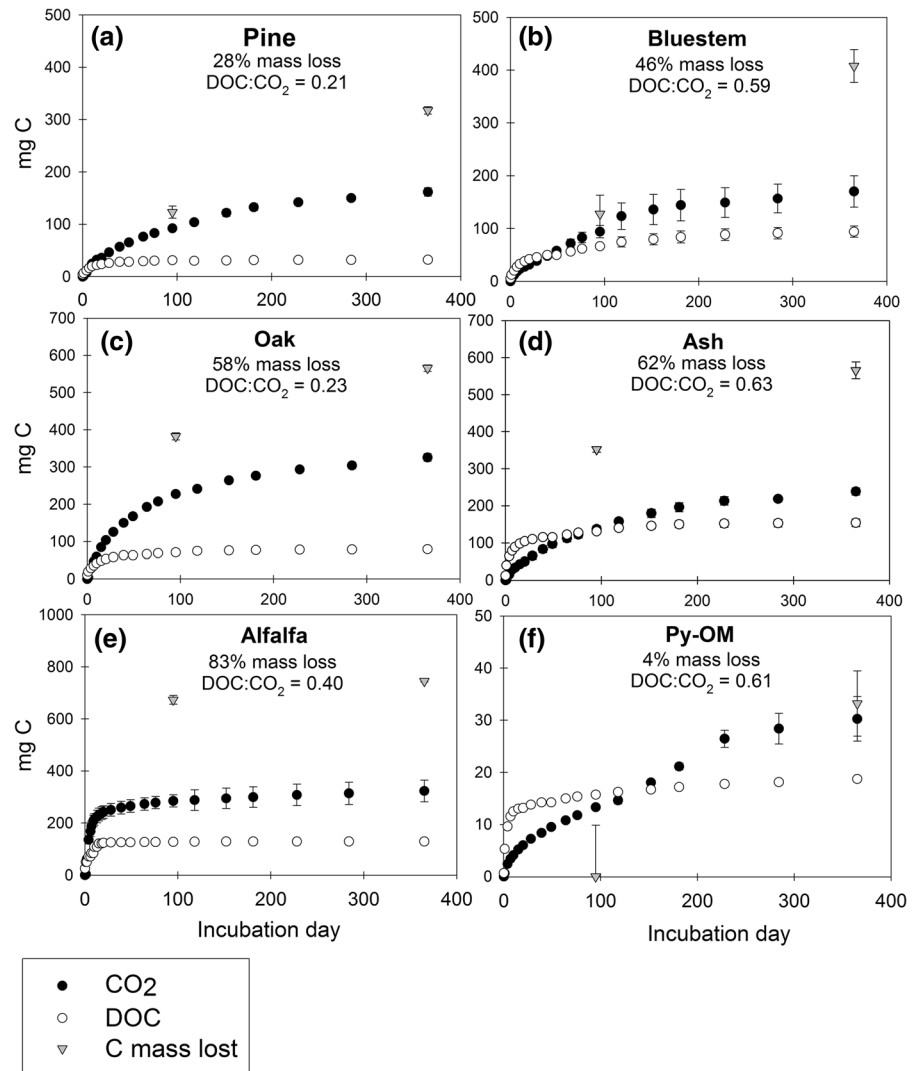
Litter	Time	Mass (g)	% C	% N	DOC (mg)	TDN (mg)	CO <sub>2</sub> (mg)	% AUR <sup>+</sup>	% $\alpha$ -Cellulose <sup>+</sup>	% Non-structural	% HWE-C
Alfalfa	Day 0	2.00 (<0.001)	44.1 (0.026)	4.09 (0.012)	NA	NA	NA	4.66 (0.432)	14.2 (0.418)	74.7 (0.308)	28.3 (0.676)
	Day 95	0.466 (0.040)	42.5 (0.218)	4.49 (0.086)	128 (4.04)	22.7 (0.875)	279 (23.7)	17.8 (1.18)	15.9 (0.651)		
	Day 365	0.333 (0.013)	38.0 (0.508)	4.21 (0.171)	129 (2.14)	25.6 (0.184)	282 (39.6)	23.2 (NA)	15.1 (NA)		
Ash	Day 0	2.00 (<0.001)	46.5 (0.608)	0.88 (0.012)	NA	NA	NA	9.81 (0.188)	19.1 (0.256)	69.0 (0.344)	25.4 (0.213)
	Day 95	1.13 (0.015)	50.6 (0.120)	1.55 (0.086)	131 (3.83)	1.75 (0.071)	123 (9.25)	33.7 (2.77)	20.9 (3.485)		
	Day 365	0.753 (0.048)	47.4 (0.797)	1.85 (0.134)	154 (10.2)	2.32 (0.289)	223 (10.1)	36.5 (NA)	17.2 (NA)		
Bluestem	Day 0	2.00 (<0.001)	44.1 (0.049)	0.478 (0.003)	NA	NA	NA	8.42 (0.522)	33.4 (0.567)	32.9 (0.266)	11.2 (0.348)
	Day 95	1.59 (0.066)	47.0 (0.263)	0.593 (0.025)	66.2 (3.83)	0.924 (0.046)	83.9 (10.8)	19.9 (1.14)	32.9 (0.289)		
	Day 365	1.09 (0.075)	43.2 (0.097)	0.487 (0.025)	93.9 (10.6)	1.29 (0.079)	160 (28.0)	19.9 (NA)	32.3 (NA)		
Py-OM	Day 0	2.00 (<0.001)	59.2 (1.021)	2.11 (0.043)	NA	NA	NA	NA	NA	11.5 (0.713)	2.10 (NA)
	Day 95	2.00 ( $8 \times 10^{-4}$ )	64.7 (0.443)	2.46 (0.185)	15.7 (0.206)	0.393 (0.017)	12.2 (0.527)	93.7 (5.07)	NA		
	Day 365	1.93 (0.004)	62.0 (0.309)	2.07 (0.119)	18.7 (0.252)	0.542 (0.009)	29.0 (4.25)	89.1 (NA)	1.60 (NA)		
Oak	Day 0	2.00 (<0.001)	47.6 (0.038)	1.32 (0.010)	NA	NA	NA	18.8 (0.259)	22.4 (0.297)	53.1 (0.591)	18.7 (2.68)
	Day 95	1.10 (0.017)	51.1 (0.165)	2.16 (0.096)	70.8 (2.89)	1.85 (0.151)	209 (3.33)	52.9 (2.28)	18.8 (1.893)		
	Day 365	0.833 (0.017)	45.7 (0.323)	2.36 (0.049)	79.4 (2.78)	2.29 (0.130)	307 (9.54)	53.0 (NA)	20.5 (NA)		
Pine	Day 0	2.00 (<0.001)	52.3 (0.049)	0.413 (0.007)	NA	NA	NA	24.4 (0.302)	22.9 (0.327)	48.3 (0.723)	9.28 (2.07)
	Day 95	1.64 (0.022)	56.6 (0.130)	0.613 (0.007)	31.3 (1.48)	0.117 (0.009)	83.9 (2.27)	68.1 (6.52)	11.9 (5.405)		
	Day 365	1.44 (0.018)	51.0 (0.185)	0.490 (0.059)	32.2 (2.35)	0.172 (0.010)	153 (8.14)	45.0 (NA)	29.0 (NA)		

Dissolved organic carbon (DOC), total dissolved nitrogen (TDN) and CO<sub>2</sub> are reported as total cumulative values over the course of the incubation

\* NA indicates that either there was not enough sample remaining to do the analysis, or that there was only enough sample for one aggregated analysis, so no standard error can be reported. For bluestem, pine and py-OM one composite sample of all three replicates was used for the day 365 lignin and cellulose determination

+ AUR = acid unhydrolyzable residue, a proximate value for lignin;  $\alpha$ -Cellulose = as determined by 73 % sulfuric acid digestion using the acid detergent fiber method (Van Soest and Wine 1968)

**Fig. 1** Substrate C losses, DOC leaching and CO<sub>2</sub> efflux dynamics over the course of the 365 day incubation of five above ground leaf litters and one pyrogenic organic matter (py-OM). *Black circles* are CO<sub>2</sub>, *open circles* are DOC, and *grey inverted triangles* are residue C lost. N = 3, error bars are standard error. Total % mass loss after 365 days and overall DOC:CO<sub>2</sub> ratios are presented



litters continued to leach some DOC after the initial period in contrast to the other litter types, which tended to level off in DOC leaching after approximately day 15 (Fig. 1).

### Three phases of DOC and CO<sub>2</sub> dynamics

Three distinct phases of decomposition were observed across all substrate types, on the basis of the DOC:CO<sub>2</sub> dynamics. The early phase, up to day 15, was characterized by very high DOC losses (~70 % of

total DOC lost) and high DOC:CO<sub>2</sub> ratios (average = 2.49, standard error = 0.830), a second or mid phase (days 16–65) was characterized by declining DOC:CO<sub>2</sub> and a third or late phase, where very little DOC was produced, was characterized by a constant DOC:CO<sub>2</sub> ratio (average = 0.370, standard error = 0.165). In examining the early decomposition phase, we found a highly significant correlation between the % HWE-C of the initial substrates and the total amount of DOC leached in the first 15 days of the incubation ( $p = 0.0017$ , Fig. 2a). The % non-

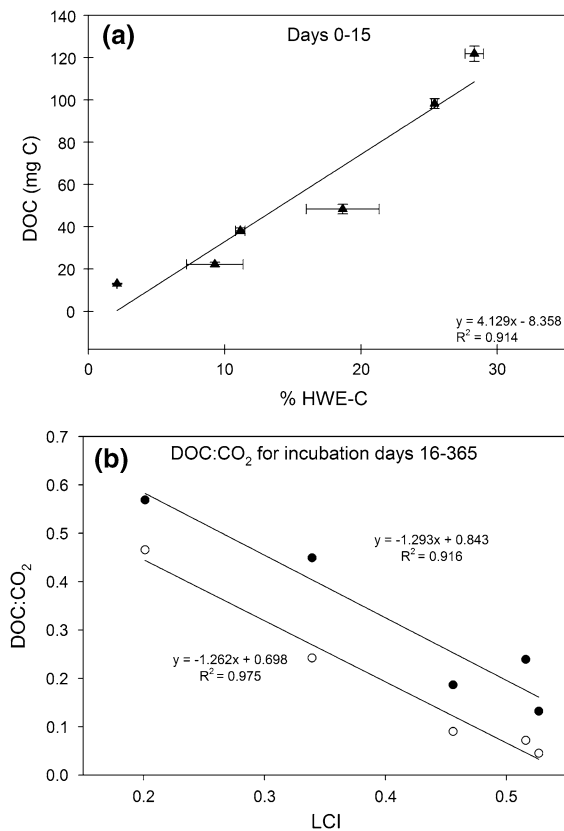


**Fig. 2** **a** Average total DOC from the early phase leaching events versus % hot water extractable carbon (HWE-C) for all five litter types and py-OM. *Bars* are standard errors ( $n = 6$  for DOC,  $n = 3$  for HWE). **b** Average DOC:CO<sub>2</sub> ratio versus initial litter LCI [lignin/(lignin +  $\alpha$ -cellulose)] for all litter types, except alfalfa, where we used the day 95 LCI ( $n = 3$ ). *Closed circles* are average DOC:CO<sub>2</sub> for days 16–64 (*mid phase*), *open circles* are average DOC:CO<sub>2</sub> for days 65–365 (*late phase*)

structural material also correlated strongly with the amount of initial DOC leaching in days 0–15 for all litter types and the py-OM, with the exception of pine litter ( $R^2 = 0.912$  without pine,  $R^2 = 0.767$  with pine).

For the mid and late stages of the incubation (days 16–64 and days 65–365) we tested several initial chemical characteristics against DOC:CO<sub>2</sub> partitioning (Table 2). We found the strongest correlation between initial LCI and the ratio of DOC:CO<sub>2</sub> losses during these phases, with the exception of day 95 LCI for alfalfa (Table 2; Fig. 2b). We assumed that the day 95 LCI for the alfalfa would better characterize the litter structural composition starting at day 16 due to its rapid decomposition, which reached its asymptote for CO<sub>2</sub> and DOC fluxes by day 15. The initial LCI still

fit for the other litter types who had not reached their asymptote for CO<sub>2</sub> and DOC fluxes by day 16. We divided the mid and late phases of decomposition based on the different offsets of the DOC:CO<sub>2</sub> versus LCI curves for these two phases (Fig. 2b). We omitted the py-OM in Fig. 2b because we did not have enough sample for the day 0 AUR and cellulose determination.

### Litter and py-OM chemistry

The substrates studied spanned a broad range of initial chemistries based on C:N, %  $\alpha$ -cellulose, % AUR, % non-structural material and % HWE-C (Table 1). Alfalfa represented the most labile litter type due to its rapid mass loss, high N content, low AUR content and low LCI of 0.24. Oak and pine had a high initial LCI of 0.46 and 0.51 respectively, while ash and bluestem both had a low LCI of 0.34 and 0.20 respectively. The initial substrates also ranged in their initial % non-structural composition, from 73.62 % (alfalfa) to 11.46 % (py-OM) (Table 1). The initial % HWE-C varied proportionally to the % non-structural composition ( $R^2 = 0.99$ ,  $p < 0.0001$ ; Table 1).

The C:N of alfalfa and py-OM did not change significantly throughout the incubation, while the C:N of ash, bluestem and oak significantly decreased between day 0 and 95 but then remained constant between day 95 and 365. The only litter type whose C:N continued to decrease both from day 0 to 95 and from day 95 to 365 was pine ( $p < 0.01$ ).

Results from the ADF digestion of the litter at all three time points revealed an increase in the AUR fraction over time, in both absolute terms and in terms of its relative contribution to the mass remaining (Table 1). Alfalfa was the only litter type whose absolute amount of the AUR did not change over time. For ash, bluestem, oak and pine the absolute mass of AUR increased on average by 190 % from day 0 to 95, and then decreased by on average 69 % from day 95 to 365. The  $\alpha$ -cellulose fraction decreased over time, both in relative and absolute amounts for all substrates (Table 1). The three replicates of the pine sample had to be aggregated for the day 365 ADF digestion, so there was no statistical power to the increase in  $\alpha$ -cellulose for pine from day 95 to day 365 (Table 1). There was not enough day 0 py-OM for initial AUR and  $\alpha$ -cellulose determination, but from day 95 to 365

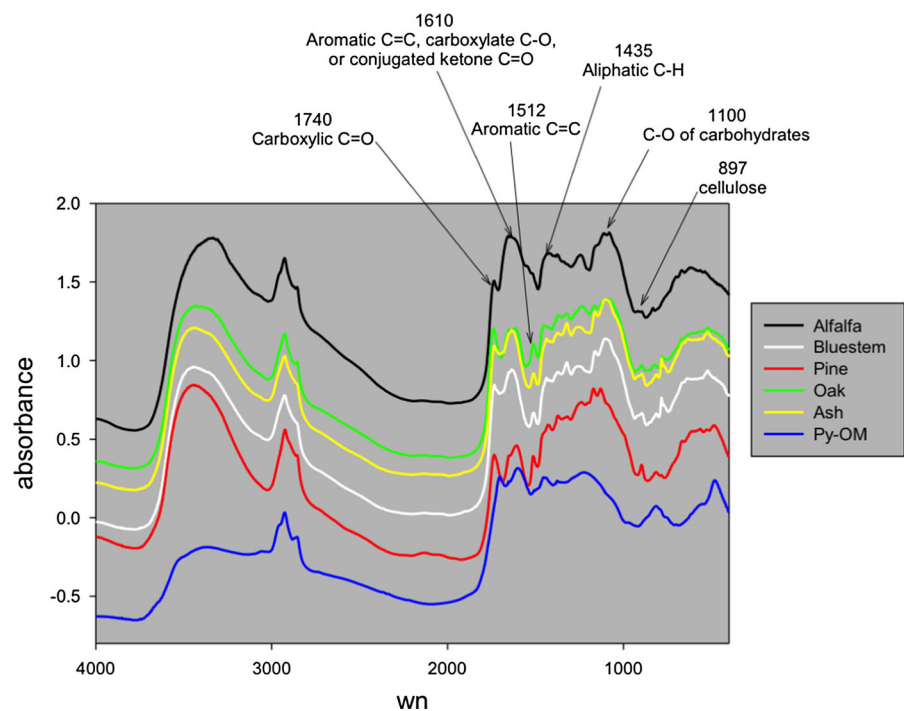


**Table 2** Regression results from the average day 16–365 proportion of C lost as DOC:CO<sub>2</sub> against various initial litter chemistry parameters on three replicates

	R <sup>2</sup>	F-value	p value
Day 0 LCI, with day 95 LCI for alfalfa*	0.9724	105.626	0.001964
Day 0 % $\alpha$ -cellulose	0.6172	4.837048	0.115244
Day 0 % non-structural	0.3479	1.600248	0.295198
Day 0 LCI	0.317	1.392538	0.323027
Day 0 %N	0.3066	1.326557	0.332878
Day 0 % lignin	0.1186	0.403701	0.570334
Day 0 lignin:N	0.0128	0.039007	0.856059

\* This is the regression shown in Fig. 2b

**Fig. 3** FTIR spectra of the initial litters and py-OM before the incubation. Absorbance is unitless and the spectra were stacked for better visualization



the absolute mass of the  $\alpha$ -cellulose fraction decreased by 50 %, while the absolute mass of the AUR fraction decreased by 3 %.

Although we did not use FTIR to quantify changes in litter chemistry, results from the FTIR analysis of the substrates at day 0, day 95 and day 365 revealed shifts in chemical composition among the substrates and over time. Initially, the py-OM samples differed significantly in chemical composition from the five litter types ( $p < 0.05$ , Fig. 3). When we removed the py-OM from our initial sample dbRDA analysis, there

was still a statistically significant difference between the five remaining litter types ( $p < 0.05$ ). This difference was mainly driven by the differences between the alfalfa and bluestem litters. At time zero, the litters had defined bands at  $\sim 3400$ , 2950–2850, 1650–1580, 1435, 1100, and 897  $\text{cm}^{-1}$  (Fig. 3). The region between 3600 and 2850 was very similar between the litters, except for the more pronounced absorbance of the pine litter at the aliphatic CH band (2950–2850  $\text{cm}^{-1}$ ), possibly because of the presence of resinous material. The py-OM had reduced

**Fig. 4** Spectral subtraction of the mid-infrared FTIR spectra from the initial litters minus decomposed litters. The subtraction spectra were stacked for better visualization. *Upward peaks* denote bands that were consumed during decomposition

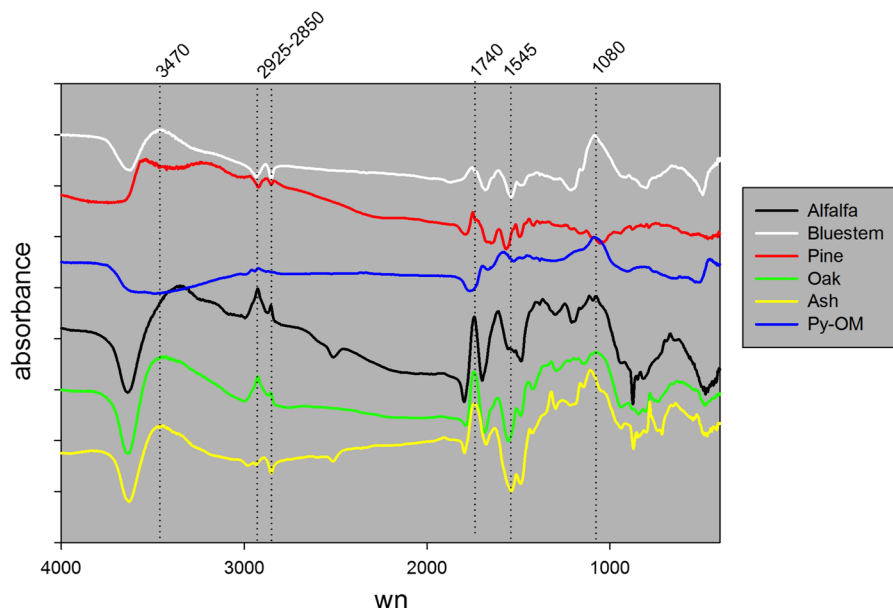
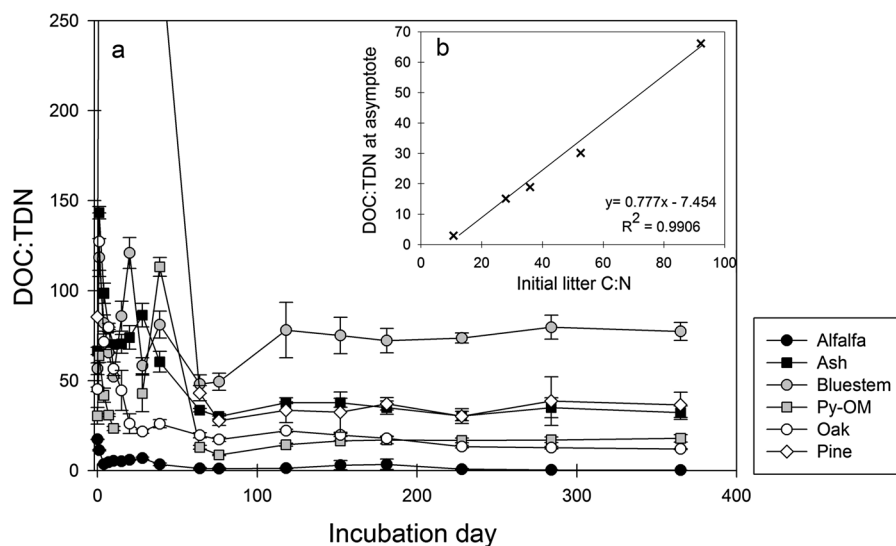


**Fig. 5 a** DOC:TDN ratio for all fresh and pyrolyzed litters over the course of the incubation. *Bars* are standard error bars,  $N = 6$  for days 0–95 and  $N = 3$  for days 96–365. *Y-axis* scale is reduced to better display the DOC:TDN dynamics, cutting of the initial phase very high DOC:TDN of the pine. **b** Regression of initial litter C:N versus average DOC:TDN of the asymptote for all aboveground plant input types except pine



absorbance at  $\sim 3400$  cm due to the loss of OH and NH groups during pyrolysis. Oak and pine had the most marked carbonyl peaks at  $1740$   $\text{cm}^{-1}$ . The peak between  $1650$  and  $1580$  narrowed towards  $1610$  in the py-OM and the pine indicating higher aromatic skeletal vibrations, whereas the alfalfa had a peak towards  $1655$  consistent with esters in proteins (Galletti et al. 1993). Between  $1500$  and  $1510$   $\text{cm}^{-1}$ , the lignin peak (White et al. 2011) was absent in the alfalfa spectrum, consistent with the high non-

structural character of this litter (Table 1; Fig. 3). Spectral subtractions showed that for all of the substrates, except for pine, there was a loss in absorbance during the incubation at  $\sim 3470$ ,  $2925$ – $2850$ ,  $1740$  and  $1080$   $\text{cm}^{-1}$ , consistent with the loss of carbonyl-containing moieties and aliphatic CH (Fig. 4). Pine, in contrast, showed a reduction in absorbance at  $3570$  and  $2940$ – $2850$   $\text{cm}^{-1}$  during incubation. The substrates tended to gain absorbance at  $1680$  and  $1545$   $\text{cm}^{-1}$  during the incubation, which

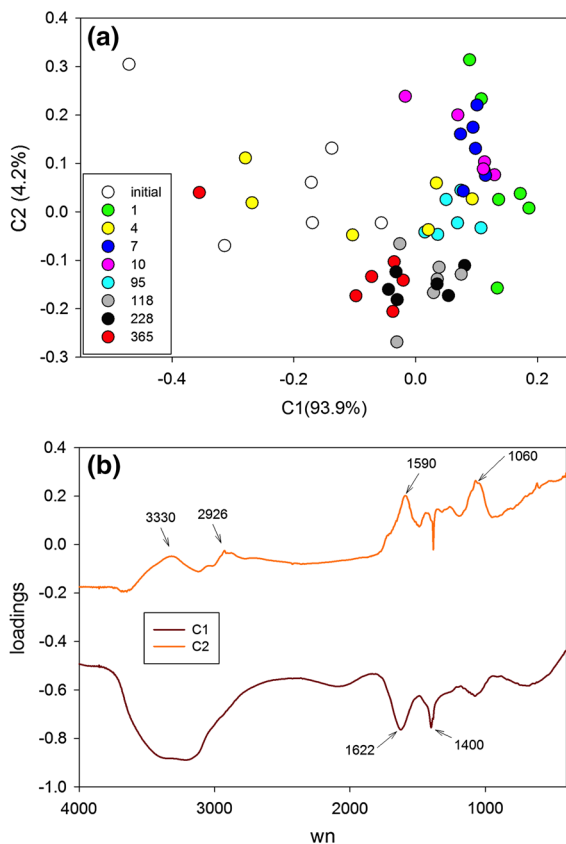


**Fig. 6** PCA scores (a), and component loading (b) results of FTIR functional group chemistry of all litter DOM leachates over time labeled by incubation day number. The percent variation accounted for by each component is in parenthesis

suggests an increase of amide and aromatic C=C during decomposition (Calderon et al. 2006).

#### Litter and py-OM chemistry controls on DOM composition over time

In addition to quantifying the substrate chemistry controls on the amount of DOC leached over time, we also measured changes in DOM DOC:TDN, organic and inorganic N composition, and functional group chemistry over time. Initially, the DOC:TDN of the DOM significantly correlated to the C:N of the initial litter ( $R^2 = 0.7967$ ,  $p = 0.017$ ). All of the DOC:TDN ratios of the DOM decreased exponentially until they reached a constant level, with the DOC:TDN of alfalfa DOM leveling off at 2.9 by day 4, oak at 18.9 by day 20, ash at 30.2 by day 64, bluestem at 66.2 by day 64, py-OM at 15.1 by day 64 and pine at 31.0 by day 64

(Fig. 5a). These ultimate DOC:TDN values of the DOM also correlate strongly with initial substrate C:N ( $R^2 = 0.9906$ ), when the pine litter is excluded (Fig. 5b). Throughout the incubation over 80 % of the TDN in the DOM was organic, i.e. not  $\text{NH}_4^+$  or  $\text{NO}_3^-$ , except for alfalfa, whose DOM contained 40–60 % inorganic N from day 28 to 365 (data not shown).

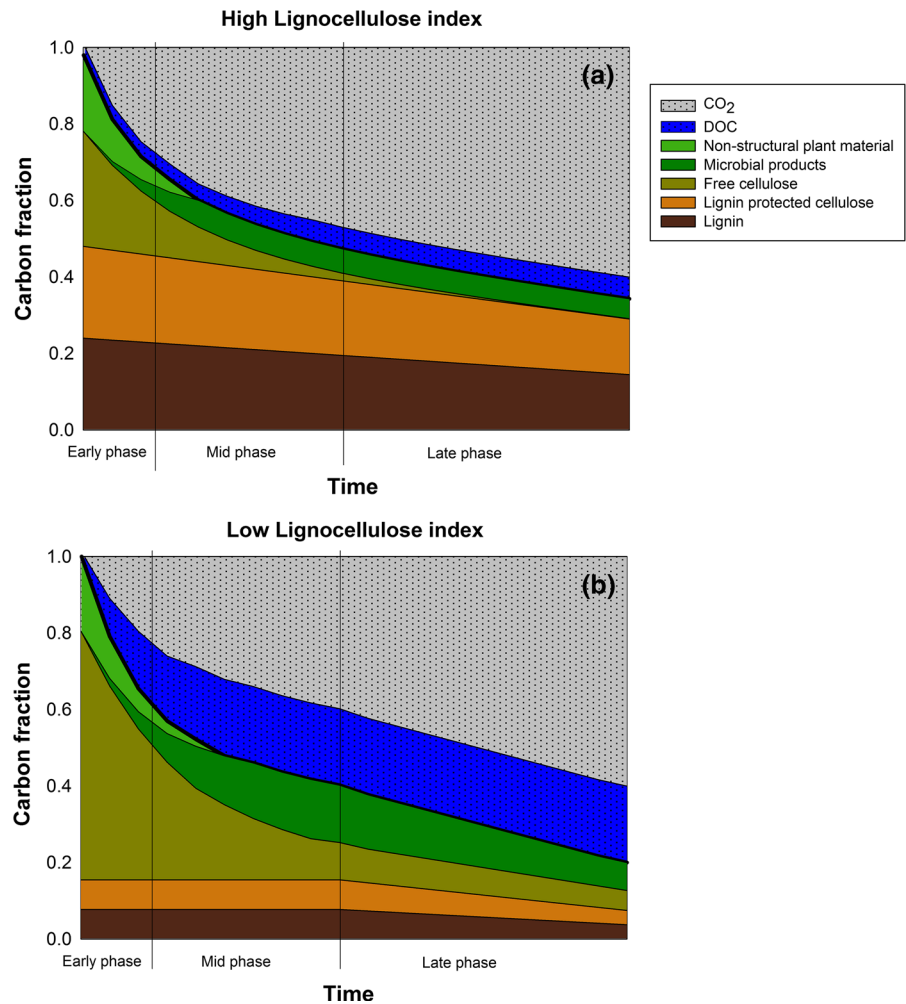
We analyzed the FTIR spectral data from nine of the leaching events during the incubation, on days 0, 1, 4, 7, 10, 95, 118, 228 and 365, by dbRDA and PCA. When we compiled the leachate FTIR data by substrate over time, we found no significant differences in the overall composition of the leachate between the different substrates according to dbRDA ( $p = 0.074$ ). The leachates showed absorbance peaks at 330, 2926, 1590, and 1060  $\text{cm}^{-1}$ . Instead, across all litter types (excluding the py-OM), dbRDA analysis showed that there was a statistically significant shift in the chemical composition of the leachate over time ( $p = 0.005$ ). Analysis of the FTIR spectra data shows that the absorbance at 3400 (OH/NH), 2070 and 1622  $\text{cm}^{-1}$  (aromatic, carboxylate, conjugated ketone C=O) decreased from days 0 and 4 to days 7 and 10 according to component 1 of the PCA (Fig. 6). Absorbance at wavenumber 2926 (aliphatic CH), 1590 (amide II) and 1060  $\text{cm}^{-1}$  (polysaccharide) decreased later in the incubation. The day 1 leachate resembled the day 7 and 10 leachate more closely than the day 0 and day 4 leachates (Fig. 6). We speculate that this is due to the presence of excess inoculum-derived DOM at day 1, which was added after the initial day 0 leaching event, being leached out along with the day 1 substrate leachate.

## Discussion

### DOM production and DOM:CO<sub>2</sub> partitioning during decomposition

After 365 days of incubation, we found that a significant fraction of the mass lost from the fresh and pyrolyzed litters was lost as DOM. Total DOC losses ranged from 2 to 16 % of the initial C, and did not correlate with rates of mass loss. This range of DOC leaching falls at the lower end of those found in previous laboratory leaching studies (Magill and Aber 2000; Kiikkila et al. 2012). It is important to note,

**Fig. 7** A new conceptual model of the relative distribution of C in decomposing litter components (non-structural compounds, microbial products produced during decomposition, free cellulose, lignin protected cellulose and lignin), dissolved organic C (DOC) and CO<sub>2</sub>, over time during decomposition of aboveground plant inputs to soil with **a** high LCI = [lignin/(lignin +  $\alpha$ -cellulose)] or **b** low LCI index. The C fraction remaining in litter components and DOC soil, while the C fraction in CO<sub>2</sub> is lost to the atmosphere



however, that laboratory litter leaching estimates may differ based on the method of leaching employed (Soong et al. 2014), and provide a measure of potential DOC leaching rather than a measure of actual DOC leaching in situ. Confirming our first hypothesis, DOC leaching rates did not correlate with CO<sub>2</sub> production rates when examined over the entire course of the incubation (Fig. 1). Similar results were found by Klotzbucher et al. (2011), who proposed that excess soluble C in the early stage accounts for the disconnect between DOC leaching and C mineralization, and that soluble C availability limits CO<sub>2</sub> production in the later stages of decomposition. We also found that the direct leaching of soluble C in the early decomposition stage accounts for the disconnect between DOC and CO<sub>2</sub> production, but we propose that litter chemistry,

in particular the initial litter LCI and potentially N availability, control the relationship between DOC leaching and C mineralization in the later stages of decomposition.

The results of our incubation suggest that substrate chemistry controls the amount of litter-C lost to DOC leaching and CO<sub>2</sub> efflux during decomposition. In Fig. 7, we present our conceptual model of decomposition that describes changes in litter chemistry controls on the early, fast phase of decomposition (based on days 0–15 of our incubation) characterized by high DOC and CO<sub>2</sub> fluxes, and the mid and late slow phases (based on days 16–64 and 65–365 of our incubation) characterized by lower DOC and CO<sub>2</sub> fluxes (Fig. 1). Solid sections represent leaf litter components, while dotted sections represent the fate of

that mass into DOC (blue) or CO<sub>2</sub> (grey). “Non-structural plant material” represents the initially leachable fraction of the litter that correlated with HWE-C in our incubation (based on Fig. 2a). “Microbial products” and “Lignin” together represent the AUR dynamics found in our study, assuming that initial day 0 measures of AUR did not contain any microbially produced secondary compounds, while measurements at day 95 and day 365 did. We divided the  $\alpha$ -cellulose fraction that we measured using the ADF method into “Free cellulose” and “Lignin protected cellulose” based on the initial lignocellulose index of the substrates.

During the early phase (day 0–15) of the incubation the amount of HWE-C, or non-structural material, in the initial substrates predicted DOC leaching (Fig. 2a). On average, 22 % of the HWE-C was leached out in the early phase. HWE-C is a measure of the water-soluble fraction of litter and has been suggested to be readily mineralizable, and consist mainly of soluble carbohydrates (Landgraf et al. 2006). HWE-C may be a more applicable metric than % non-structural material as measured by the NDF procedure for estimating the early phase DOC leaching, due to the wide range of NDF procedure modifications throughout the literature and the inclusion of lipids in the NDF fraction (Van Soest et al. 1991). In our study, %HWE-C did not correlate as well with CO<sub>2</sub> mineralization during the initial phase ( $R^2 = 0.67$ ) as it did with DOC leaching ( $R^2 = 0.914$ ), and so should be considered an even better predictor of leachable C than of readily mineralizable C in fresh litter samples. The reflection of initial litter C:N in the initial high DOC:TDN ratios, as well as the lack of correlation between DOC and CO<sub>2</sub> during the early phase of decomposition, provide evidence that in this early phase DOM consists of soluble plant material, not microbial products (Fig. 5).

During the mid and late phases of decomposition (day 16–64 and day 65–365), the initial litter LCI controlled partitioning of C loss to DOC and CO<sub>2</sub> fluxes (Fig. 2b). The LCI has historically been a good predictor of litter mass loss rates (Preston et al. 2009a), but to our knowledge this is the first time it has been shown to control the ratio of mass lost to DOC:CO<sub>2</sub>. We propose that the higher DOM leaching from litters, such as bluestem and ash with a low LCI, is mainly due to leaching from unprotected cellulose, whereas the higher CO<sub>2</sub> production from litters, such as pine and

oak with high LCI, is due to lignin protection of cellulose decomposition (Fig. 7). The mid and late phases showed different DOC:CO<sub>2</sub> losses, with higher DOC:CO<sub>2</sub> losses during the mid phase (Fig. 2b). The higher intercept of the curve for the mid phase (days 16–64) is likely due to the availability of unprotected cellulose (Figs. 2b, 7), which has a high CUE leading to more DOC production (Moorhead et al. 2013). During the late phase (days 65–365) there is more CO<sub>2</sub> production relative to DOC than the mid phase due to the lower energy yield from the decomposition of remaining lignin and lignin-protected cellulose (Moorhead et al. 2013) (Figs. 2b, 7). The similar slope of the relationship between LCI and DOC:CO<sub>2</sub> losses during the mid and late phases demonstrates the LCI controls on DOC:CO<sub>2</sub> partitioning once the initial plant soluble fraction has been leached (Figs. 2b, 7). For low LCI material, as free cellulose is broken down and leached during the mid-phase the remaining residue begins to resemble the high LCI material, so CUE is lower during the late phase as lignin and lignin protected cellulose are degraded resulting in higher CO<sub>2</sub> losses (Fig. 7).

Our results are consistent with the Moorhead et al. (2013) model of the relationship between LCI and CUE during litter decomposition. In accordance with their model, our results show that at a higher LCI there is a higher energetic cost to the breakdown of the litter structural material and more C is lost as CO<sub>2</sub>, whereas at lower LCI the excess energy from unprotected cellulose breakdown causes more C to be leached as DOC. Ash and bluestem, both characterized by low LCI, continued to have high DOC leaching throughout the mid and late phases of the incubation, likely due to the high availability of unprotected cellulose (Figs. 1, 7). The alfalfa litter was the one exception to this trend; when using the initial LCI value, alfalfa did not fit the DOC:CO<sub>2</sub> trend exhibited by other litters in later stages of decomposition, however alfalfa did fit this trend when its day 95 LCI was used (Fig. 2b; Table 2). This can be explained by the fact that alfalfa was the only litter type in our study that is not N limited (Table 1). Abundant N availability can reduce DOC leaching due to higher C immobilization in microbial residues (e.g., higher microbial CUE), leading to a lower DOC leaching than would be expected based on LCI (Sinsabaugh et al. 2013; Manzoni et al. 2012). For N-limited material such as ash, bluestem, oak and pine, N did not control DOC leaching, rather LCI

controlled CUE and the partitioning between DOC and CO<sub>2</sub> fluxes. Under field conditions external N inputs could add N to decomposing plant material, and thus the interaction between N availability and LCI controls on DOC leaching in situ is an important area of future research.

Approximately 30 % of the C lost from all of the litter types in our incubation was not accounted for as DOC or CO<sub>2</sub>. This could be due to a leaking of unaccounted for CO<sub>2</sub> from the jars, or possibly from the emission of unmeasured volatile organic compounds (Gray and Fierer 2012) and methane from the decomposing litter. We could not confirm that all of the missing C was lost as CO<sub>2</sub>, so did not include it in our measurements of CO<sub>2</sub> flux, but when added to the CO<sub>2</sub> flux we found the same significant LCI control over the ratio of DOC:CO<sub>2</sub> losses during the mid and late phases ( $R^2 = 0.85$  for day 16–64, and  $R^2 = 0.96$  for day 65–365).

#### DOC and CO<sub>2</sub> fluxes from pyrogenic organic matter

Depending on feedstock and pyrolysis conditions, chemical properties and biodegradability of py-OM may differ significantly (Baldock and Smernik 2002). During our incubation of py-OM produced from pyrolysis of *A. gerardii* at 300 °C for 4 h, we found an overall non-statistically significant mass loss of 4 %. Of the initial C in the py-OM, 1.57 % was lost as DOC and 2.59 % was lost as CO<sub>2</sub>. These values are similar to the 1 % DOC and 2.2 % CO<sub>2</sub> losses found in a field study from py-OM leaching in a savanna Oxisol (Major et al. 2010). Similarly to non-pyrolyzed litters, nearly all the DOC leached from py-OM in the early phase of decomposition (day 0–15). This points toward the need for a two-phase model of py-OM decomposition with a fast early stage and a much slower later stage (Foereid et al. 2011). The implications of py-OM DOM inputs to the soil after a fire depend on complex DOM-soil interactions, but could increase soil fertility in some circumstances (Novak et al. 2009). HWE-C is a good measure of the leachable fraction of py-OM, with 75 % of the total DOC leaching from py-OM occurring in the early phase, accounting for 20 % of the HWE-C, similar to the litter dynamics (Fig. 2a). By day 95, the LCI of the py-OM was 0.97, with CO<sub>2</sub> fluxes greatly outweighing DOC fluxes (Fig. 1). Although py-OM decomposition

is slow, this study confirms the idea that, in soils, py-OM may behave similarly to non-pyrolyzed litter (Knicker 2011). Thus, py-OM chemistry could be used to predict the proportional loss of py-OM to leaching or respiration, and may help explain the variable estimates of py-OM mean residence times in soils (Schmidt et al. 2011), as well as better inform projections of fire impacts on ecosystem C cycling.

#### Substrates and DOM chemistry changes during decomposition

The cellulose and AUR chemistry of the different substrates changed progressively throughout the incubation (Table 1). Alfa-cellulose content declined throughout the incubation, while AUR content increased from day 0 to 95 then decreased from day 95 to 365 (Table 1). Our observations of increasing absolute AUR amounts are consistent with the concept of AUR as a measurement that contains not only lignin but also secondary compounds, or microbial products, produced during decomposition (Preston et al. 1997; Johansson et al. 1986). We took efforts to ensure that our litter samples had not touched the ground or been rained on prior to collection, so the initial AUR values used to calculate the initial LCI are a good estimate of initial lignin content. The increase in AUR at day 95 (Table 1) could be due to the production of secondary compounds from high microbial activity (i.e. CO<sub>2</sub> flux) during the early and mid-phases of decomposition (Fig. 7). While the AUR fraction cannot be used to infer lignin dynamics during decomposition (Cotrufo et al. 2013), our results suggest that this recalcitrant fraction is a key regulator of DOC:CO<sub>2</sub> partitioning from decomposing plant material, and that the AUR fraction is relevant to calculating LCI.

The leachate chemistry changed during the course of the incubation reflecting the progressive loss of non-structural plant material followed by the breakdown products of cellulose and microbial products (Fig. 6). The decline in DOC:TDN throughout the incubation indicates that leaching is initially plant-derived and later is comprised of a mixture of plant decay products and some microbial products (Fig. 5). Although microbial products were being produced during the incubation, as indicated by the accumulation of AUR, these low C:N microbial products (Cleveland and Liptzin 2007) did not appear to be the dominant component of DOM due to the high

asymptote of the DOC:TDN ratios toward the end of the incubation and their correlation with litter C:N (Fig. 5). Substrates such as bluestem and ash, with a large cellulose fraction and higher rates of DOM leaching in the mid and late phases, had the highest DOC:TDN ratios at their asymptotes reflecting the continual leaching of the cellulose degradation products from these low LCI litter types (Fig. 5a). The leachate from all of the substrates except alfalfa contained mainly organic N with very little  $\text{NH}_4^+$  and  $\text{NO}_3^-$ . The low C:N of the alfalfa leachate, along with the presence of  $\text{NH}_4^+$  and  $\text{NO}_3^-$ , provide evidence that all of the substrates except alfalfa were N limited, and thus fit the proposed LCI model (Fig. 7). Over time, all of the litters except pine lost absorbance at  $\sim 3400$ ,  $2925$ – $2850$ ,  $1740$  and  $1080 \text{ cm}^{-1}$ , consistent with the loss of carbohydrates, aliphatic CH, and progression of decomposition state (Haberhauer et al. 1998).

The functional group chemistry of the DOM reflects the sequential changes in substrate chemistry over time (hypothesis 2). DOM functional group chemistry changed significantly with time across all substrate types. DOM functional group chemistry became more similar over time (Fig. 6), indicating that the effect of initial substrate chemistry (Fig. 3) on DOM composition decreases as litter chemistry converges with increasing decomposition (Preston et al. 2009a). Initially (day 0–10), the DOM showed high absorbance of OH/NH ( $3400 \text{ cm}^{-1}$ ), aromatic, carboxylate and conjugated ketone C=O ( $2070$  and  $1622 \text{ cm}^{-1}$ ) functional groups (Fig. 6). This is also when most of the leaching occurred. Although microbial degradability of DOM is high (Don and Kalbitz 2005), it is possible that some leachate from aboveground plant materials could reach mineral soils without being transformed (Kalbitz et al. 2005). Carbohydrates (–OH) in the initial DOM have limited sorption potential to mineral components in the soil (Oren and Chefetz 2012). Carboxylic groups at  $1622 \text{ cm}^{-1}$ , however have been shown to play a major role in the binding of OM to metal oxides, and could be directly stabilized onto the minerals in the soil, especially under high pH conditions (Oren and Chefetz 2012; Kaiser and Guggenberger 2000). Later (day 95–365), the DOM showed absorbance indicative of mainly aliphatic CH ( $2926 \text{ cm}^{-1}$ ), amide II ( $1590 \text{ cm}^{-1}$ ) and polysaccharide (C–O,  $1060 \text{ cm}^{-1}$ ) functional groups (Fig. 6). These DOM functional groups may be indicative of later stage decomposition

products such as waxes [ $2926 \text{ cm}^{-1}$ , (White et al. 2011)], lignin degradation products [ $1590 \text{ cm}^{-1}$ , (Calderon et al. 2006)] and polysaccharides with limited mineral sorption potential [ $1060 \text{ cm}^{-1}$ , (Oren and Chefetz 2012)]. Therefore leaching of aromatic structures and carboxyl groups ( $1622 \text{ cm}^{-1}$ ) in the early phase of decomposition could contribute significantly to soil C stabilization through ligand exchange reactions with metal oxide surfaces in the soil (Kaiser and Guggenberger 2000). Since HWE-C correlates strongly with early phase DOC leaching, HWE-C could be a good metric for estimating litter leachate contributions to SOM formation across different plant species.

### Implications and conclusions

During our 365 day incubation, we found that up to 16 % of litter mass was lost as DOC, up to 37 % was lost as  $\text{CO}_2$ , and that litter chemistry controlled this partitioning (hypothesis 1). The large amount of DOM leaching from decomposing fresh and pyrolyzed plant litters can be used to help estimate aboveground plant inputs to the soil and SOM formation. Our finding that substrates with a larger HWE-C fraction and faster mass loss lose proportionally more mass to DOC than  $\text{CO}_2$ , as compared to slower decomposing substrates, provides evidence of the potential for fast decomposing litter types to contribute relatively more OM to the soil than litters that decompose more slowly (Cotrufu et al. 2013). Litter DOM inputs to the soil may also contribute more to soil C sequestration due to their high biodegradability by soil microbes (Kalbitz et al. 2003), whose metabolic products contribute to the most persistent SOM pools (Grandy and Neff 2008). If not immediately transformed by soil microbes, the sequential shift in functional group chemistry of DOM over the course of decomposition found here has important implications for its fate once in the soil (Oren and Chefetz 2012). A sequential change in litter chemistry during decomposition appears to control the composition of DOM leaching from litter over time (hypothesis 2). Non-microbial transformed soluble plant components from the partial breakdown of cellulose and lignin appear to leach out even during the later phases of decomposition for litters with a large cellulose fraction. The fate of DOM leached from aboveground plant material once in the soil, however depends on several factors such as pH (Oren

and Chefetz 2012), microbial community (Cleveland et al. 2007) and clay content (Wang et al. 2003) and is beyond the scope of our study.

Substrates with a high amount of non-structural material leached more DOC initially during the high leaching period, and litters with a low LCI leached more DOC relative to CO<sub>2</sub> during the later lower leaching period (Fig. 2). These relationships provide the basis for our new conceptual model on how litter chemistry can be used to predict the fate of litter mass loss (Fig. 7), which is an advancement over previous models focusing only on controls of mass loss rates (Berg and Matzner 1997; Chapin et al. 2002). Under field conditions, climate largely controls litter decomposition rates (Aerts 1997) and we did not test the role of climate in the DOC:CO<sub>2</sub> partitioning. However the specific litter chemical mechanisms controlling DOC and CO<sub>2</sub> fluxes found here can be used to start building and testing models of litter decomposition and aboveground plant material–soil–atmosphere C cycling under field conditions. We propose that these highly significant litter chemistry controls on DOC leaching and CO<sub>2</sub> efflux should be incorporated into mathematical models of ecosystem C cycling to account for the fluxes of C from decomposing plant material to the soil and atmosphere.

**Acknowledgments** This work would not have been possible without help from D. Rutherford at USGS, C. Rhodes and D. Pierson at USFS, K. Guilbert, D. Reuss, C. Pinney, J. Botte, and M. Jurich at Ecocore. The work was funded by the NSF-DEB grant #0918482, the NSF Graduate Research Fellowship Program and the NSF Research Experience for Teacher program. The analytical work was carried out at the EcoCore analytical services facility at Colorado State University (<http://ecocore.nrel.colostate.edu/>).

## References

Aber JD, Melillo JM, McLaugherty CA (1990) Predicting long-term patterns of mass-loss, nitrogen dynamics, and soil organic-matter formation from initial fine litter chemistry in temperate forest ecosystems. *Can J Bot-Revue Can Bot* 68(10):2201–2208

Adair EC, Parton WJ, Del Grosso SJ, Silver WL, Harmon ME, Hall SA, Burke IC, Hart SC (2008) Simple three-pool model accurately describes patterns of long-term litter decomposition in diverse climates. *Glob Change Biol* 14(11): 2636–2660. doi:10.1111/j.1365-2486.2008.01674.x

Aerts R (1997) Climate, leaf litter chemistry and leaf litter decomposition in terrestrial ecosystems: a triangular relationship. *Oikos* 79(3):439–449. doi:10.2307/3546886

Baldock JA, Smernik RJ (2002) Chemical composition and bioavailability of thermally, altered *Pinus resinosa* (Red Pine) wood. *Org Geochem* 33(9):1093–1109

Berg B, Matzner E (1997) Effect of N deposition on decomposition of plant litter and soil organic matter in forest systems. *Environ Rev* 5(1):1–25. doi:10.1139/a96-017

Berg B, McLaugherty C (2003) Plant litter. Decomposition, humus formation, carbon sequestration. Springer, Berlin

Bocock KL, Gilbert OJW (1957) The disappearance of leaf litter under different woodland conditions. *Plant Soil* 9(2): 179–185. doi:10.1007/BF01398924

Calderon FJ, McCarty GW, Reeves JB (2006) Pyrolysis-MS and FT-IR analysis of fresh and decomposed dairy manure. *J Anal Appl Pyrol* 76(1–2):14–23. doi:10.1016/j.jaap.2005.06.009

Chapin FS, Matson PA, Mooney HA (2002) Principles of terrestrial ecosystem ecology. Springer, New York

Cleveland CC, Liptzin D (2007) C : n : P stoichiometry in soil: is there a “Redfield ratio” for the microbial biomass? *Biogeochemistry* 85(3):235–252. doi:10.1007/s10533-007-9132-0

Cleveland CC, Nemergut DR, Schmidt SK, Townsend AR (2007) Increases in soil respiration following labile carbon additions linked to rapid shifts in soil microbial community composition. *Biogeochemistry* 82(3):229–240. doi:10.1007/s10533-006-9065-z

Cotrufo MF, del Galdo I, Piermatteo D (2009) Litter decomposition: concepts, methods and future perspectives. In: Kutsch WL, Bahn M, Heinemeyer A (eds) Soil carbon dynamics: an integrated methodology. Cambridge University Press, Cambridge, pp 76–90

Cotrufo MF, Wallenstein MD, Boot CM, Deneff K, Paul E (2013) The Microbial Efficiency-Matrix Stabilization (MEMS) framework integrates plant litter decomposition with soil organic matter stabilization: do labile plant inputs form stable soil organic matter? *Glob Change Biol* 19(4): 988–995. doi:10.1111/gcb.12113

Coûteaux M-M, Mousseau M, Célérier M-L, Bottner P (1991) Increased atmospheric CO<sub>2</sub> and litter quality: decomposition of sweet chestnut leaf litter with animal food webs of different complexities. *Oikos* 61(1):54–64. doi:10.2307/3545406

Don A, Kalbitz K (2005) Amounts and degradability of dissolved organic carbon from foliar litter at different decomposition stages. *Soil Biol Biochem* 37(12):2171–2179. doi:10.1016/j.soilbio.2005.03.019

Flannigan MD, Stocks BJ, Wotton BM (2000) Climate change and forest fires. *Sci Total Environ* 262(3):221–229. doi:10.1016/S0048-9697(00)00524-6

Foeroid B, Lehmann J, Major J (2011) Modeling black carbon degradation and movement in soil. *Plant Soil* 345(1–2): 223–236. doi:10.1007/s11104-011-0773-3

Galletti GC, Reeves JB, Bloomfield J, Vogt KA, Vogt DJ (1993) Analysis of leaf and fine-root litter from a subtropical montane rain-forest by pyrolysis-gas chromatography mass-spectrometry. *J Anal Appl Pyrol* 27(1):1–14. doi:10.1016/0165-2370(93)80018-u

Gallo ME, Lauber CL, Cabaniss SE, Waldrop MP, Sinsabaugh RL, Zak DR (2005) Soil organic matter and litter chemistry response to experimental N deposition in northern temperate deciduous forest ecosystems. *Glob Change Biol* 11(9): 1514–1521. doi:10.1111/j.1365-2486.2005.001001.x



- Grandy AS, Neff JC (2008) Molecular C dynamics downstream: the biochemical decomposition sequence and its impact on soil organic matter structure and function. *Sci Total Environ* 404(2–3):297–307. doi:[10.1016/j.scitotenv.2007.11.013](https://doi.org/10.1016/j.scitotenv.2007.11.013)
- Gray CM, Fierer N (2012) Impacts of nitrogen fertilization on volatile organic compound emissions from decomposing plant litter. *Glob Change Biol* 18(2):739–748. doi:[10.1111/j.1365-2486.2011.02569.x](https://doi.org/10.1111/j.1365-2486.2011.02569.x)
- Haberhauer G, Rafferty B, Strebl F, Gerzabek MH (1998) Comparison of the composition of forest soil litter derived from three different sites at various decompositional stages using FTIR spectroscopy. *Geoderma* 83(3–4):331–342. doi:[10.1016/s0016-7061\(98\)00008-1](https://doi.org/10.1016/s0016-7061(98)00008-1)
- He Z, Mao J, Honeycutt CW, Ohno T, Hunt JF, Cade-Menun BJ (2009) Characterization of plant-derived water extractable organic matter by multiple spectroscopic techniques. *Biol Fertil Soils* 45(6):609–616. doi:[10.1007/s00374-009-0369-8](https://doi.org/10.1007/s00374-009-0369-8)
- Hessen DO, Agren GI, Anderson TR, Elser JJ, De Ruiter PC (2004) Carbon, sequestration in ecosystems: the role of stoichiometry. *Ecology* 85(5):1179–1192. doi:[10.1890/02-0251](https://doi.org/10.1890/02-0251)
- Johansson MB, Kogel I, Zech W (1986) Changes in the lignin fraction of spruce and pine needle litter during decomposition as studied by some chemical methods. *Soil Biol Biochem* 18(6):611–619. doi:[10.1016/0038-0717\(86\)90084-2](https://doi.org/10.1016/0038-0717(86)90084-2)
- Kaiser K, Guggenberger G (2000) The role of DOM sorption to mineral surfaces in the preservation of organic matter in soils. *Org Geochem* 31(7–8):711–725. doi:[10.1016/s0146-6380\(00\)00046-2](https://doi.org/10.1016/s0146-6380(00)00046-2)
- Kaiser K, Kalbitz K (2012) Cycling downwards - dissolved organic matter in soils. *Soil Biol Biochem* 52:29–32. doi:[10.1016/j.soilbio.2012.04.002](https://doi.org/10.1016/j.soilbio.2012.04.002)
- Kalbitz K, Schmerwitz J, Schwesig D, Matzner E (2003) Biodegradation of soil-derived dissolved organic matter as related to its properties. *Geoderma* 113(3–4):273–291. doi:[10.1016/S0016-7061\(02\)00365-8](https://doi.org/10.1016/S0016-7061(02)00365-8)
- Kalbitz K, Schwesig D, Rethemeyer J, Matzner E (2005) Stabilization of dissolved organic matter by sorption to the mineral soil. *Soil Biol Biochem* 37(7):1319–1331. doi:[10.1016/j.soilbio.2004.11.028](https://doi.org/10.1016/j.soilbio.2004.11.028)
- Kalbitz K, Kaiser K, Bargholz J, Dardenne P (2006) Lignin degradation controls the production of dissolved organic matter in decomposing foliar litter. *Eur J Soil Sci* 57(4):504–516. doi:[10.1111/j.1365-2389.2006.00797.x](https://doi.org/10.1111/j.1365-2389.2006.00797.x)
- Kelly AE, Goulden ML (2008) Rapid shifts in plant distribution with recent climate change. *Proc Natl Acad Sci USA* 105(33):11823–11826. doi:[10.1073/pnas.0802891105](https://doi.org/10.1073/pnas.0802891105)
- Kiikkilä O, Kitunen V, Spetz P, Smolander A (2012) Characterization of dissolved organic matter in decomposing Norway spruce and silver birch litter. *Eur J Soil Sci* 63(4):476–486. doi:[10.1111/j.1365-2389.2012.01457.x](https://doi.org/10.1111/j.1365-2389.2012.01457.x)
- Klotzbucher T, Kaiser K, Guggenberger G, Gatzek C, Kalbitz K (2011) A new conceptual model for the fate of lignin in decomposing plant litter. *Ecology* 92(5):1052–1062
- Knicker H (2011) Pyrogenic organic matter in soil: its origin and occurrence, its chemistry and survival in soil environments. *Quatern Int* 243(2):251–263. doi:[10.1016/j.quaint.2011.02.037](https://doi.org/10.1016/j.quaint.2011.02.037)
- Lammers K, Arbuttle-Keil G, Dighton J (2009) MIR study of the changes in carbohydrate chemistry of three New Jersey pine barrens leaf litters during simulated control burning. *Soil Biol Biochem* 41(2):340–347. doi:[10.1016/j.soilbio.2008.11.005](https://doi.org/10.1016/j.soilbio.2008.11.005)
- Landgraf D, Leinweber P, Makeschin F (2006) Cold and hot water-extractable organic matter as indicators of litter decomposition in forest soils. *J Plant Nutr Soil Sci* 169(1):76–82. doi:[10.1002/jpin.200521711](https://doi.org/10.1002/jpin.200521711)
- Legendre P (1999) Anderson MJ (1999) Distance-based redundancy analysis: testing multispecies responses in multifactorial ecological experiments (vol 69, pg 1. *Ecol Monogr* 69(4):512
- Li LJ, Zeng DH, Yu ZY, Fan ZP, Yang D, Liu YX (2011) Impact of litter quality and soil nutrient availability on leaf decomposition rate in a semi-arid grassland of Northeast China. *J Arid Environ* 75(9):787–792. doi:[10.1016/j.jaridenv.2011.04.009](https://doi.org/10.1016/j.jaridenv.2011.04.009)
- Magill AH, Aber JD (2000) Dissolved organic carbon and nitrogen relationships in forest litter as affected by nitrogen deposition. *Soil Biol Biochem* 32(5):603–613. doi:[10.1016/s0038-0717\(99\)00187-x](https://doi.org/10.1016/s0038-0717(99)00187-x)
- Major J, Lehmann J, Rondon M, Goodale C (2010) Fate of soil-applied black carbon: downward migration, leaching and soil respiration. *Glob Change Biol* 16(4):1366–1379. doi:[10.1111/j.1365-2486.2009.02044.x](https://doi.org/10.1111/j.1365-2486.2009.02044.x)
- Manzoni S, Taylor P, Richter A, Porporato A, Agren GI (2012) Environmental and stoichiometric controls on microbial carbon-use efficiency in soils. *New Phytol* 196(1):79–91. doi:[10.1111/j.1469-8137.2012.04225.x](https://doi.org/10.1111/j.1469-8137.2012.04225.x)
- Melillo JM, Aber JD, Muratore JF (1982) Nitrogen and lignin control of hardwood leaf litter decomposition dynamics. *Ecology* 63(3):621–626. doi:[10.2307/1936780](https://doi.org/10.2307/1936780)
- Moorhead DL, Lashermes G, Sinsabaugh RL, Weintraub MN (2013) Calculating co-metabolic costs of lignin decay and their impacts on carbon use efficiency. *Soil Biol Biochem* 66:17–19. doi:[10.1016/j.soilbio.2013.06.016](https://doi.org/10.1016/j.soilbio.2013.06.016)
- Novak JM, Busscher WJ, Laird DL, Ahmedna M, Watts DW, Niandou MAS (2009) Impact of biochar amendment on fertility of a southeastern coastal plain soil. *Soil Sci* 174(2):105–112. doi:[10.1097/SS.0b013e3181981d9a](https://doi.org/10.1097/SS.0b013e3181981d9a)
- Oksanen J, F. G. Blanchet, R. Kindt, P. Legendre, P. R. Minchin, R. B. O'Hara, G. L. Simpson, P. Solymos, M. H. H. Stevens, and H. Wagner (2013) *Vegan Community Ecology Package*, Version 2.0-10
- Oren A, Chefetz B (2012) Sorptive and desorptive fractionation of dissolved organic matter by mineral soil matrices. *J Environ Qual* 41(2):526–533. doi:[10.2134/jeq2011.0362](https://doi.org/10.2134/jeq2011.0362)
- Osono T, Takeda H (2005) Limit values for decomposition and convergence process of lignocellulose fraction in decomposing leaf litter of 14 tree species in a cool temperate forest. *Ecol Res* 20(1):51–58. doi:[10.1007/s11284-004-0011-z](https://doi.org/10.1007/s11284-004-0011-z)
- Preston CM, Trofymow JA, Sayer BG, Niu JN (1997) C-13 nuclear magnetic resonance spectroscopy with cross-polarization and magic-angle spinning investigation of the proximate-analysis fractions used to assess litter quality in decomposition studies. *Can J Bot-Rev Can Bot* 75(9):1601–1613
- Preston CM, Nault JR, Trofymow JA (2009a) Chemical changes during 6 years of decomposition of 11 litters in some canadian forest sites. Part 2. C-13 Abundance, solid-state

- c-13 nmr spectroscopy and the meaning of “lignin”. *Ecosystems* 12(7):1078–1102. doi:[10.1007/s10021-009-9267-z](https://doi.org/10.1007/s10021-009-9267-z)
- Preston CM, Nault JR, Trofymow JA, Smyth C, Grp CW (2009b) Chemical changes during 6 years of decomposition of 11 litters in some canadian forest sites. part 1. elemental composition, tannins, phenolics, and proximate fractions. *Ecosystems* 12(7):1053–1077. doi:[10.1007/s10021-009-9266-0](https://doi.org/10.1007/s10021-009-9266-0)
- Qualls RG, Haines BL (1991) Fluxes of dissolved organic nutrients and humic substances in a deciduous forest. *Ecology* 72(1):254–266. doi:[10.2307/1938919](https://doi.org/10.2307/1938919)
- Rowland AP, Roberts JD (1994) Lignin and cellulose fractionation in decomposition studies using acid-detergent fiber methods. *Commun Soil Sci Plant Anal* 25(3–4): 269–277. doi:[10.1080/00103629409369035](https://doi.org/10.1080/00103629409369035)
- Rutherford DW, Wershaw RL, Rostad CE, Kelly CN (2012) Effect of formation conditions on biochars: compositional and structural properties of cellulose, lignin, and pine biochars. *Biomass Bioenergy* 46:693–701. doi:[10.1016/j.biombioe.2012.06.026](https://doi.org/10.1016/j.biombioe.2012.06.026)
- Santos F, Torn MS, Bird JA (2012) Biological degradation of pyrogenic organic matter in temperate forest soils. *Soil Biol Biochem* 51:115–124. doi:[10.1016/j.soilbio.2012.04.005](https://doi.org/10.1016/j.soilbio.2012.04.005)
- Schmidt MWI, Torn MS, Abiven S, Dittmar T, Guggenberger G, Janssens IA, Kleber M, Kogel-Knabner I, Lehmann J, Manning DAC, Nannipieri P, Rasse DP, Weiner S, Trumbore SE (2011) Persistence of soil organic matter as an ecosystem property. *Nature* 478(7367):49–56. doi:[10.1038/nature10386](https://doi.org/10.1038/nature10386)
- Singh N, Abiven S, Torn MS, Schmidt MWI (2012) Fire-derived organic carbon in soil turns over on a centennial scale. *Biogeosciences* 9(8):2847–2857. doi:[10.5194/bg-9-2847-2012](https://doi.org/10.5194/bg-9-2847-2012)
- Sinsabaugh RL, Manzoni S, Moorhead DL, Richter A (2013) Carbon use efficiency of microbial communities: stoichiometry, methodology and modelling. *Ecol Lett* 16(7): 930–939. doi:[10.1111/ele.12113](https://doi.org/10.1111/ele.12113)
- Soong JL, Calderon FJ, Betzen J, Cotrufo MF (2014) Quantification and FTIR characterization of dissolved organic carbon and total dissolved nitrogen leached from litter: a comparison of methods across litter types. *Plant Soil* 385:125–137. doi:[10.1007/s11104-014-2232-4](https://doi.org/10.1007/s11104-014-2232-4)
- Stewart CE, Zheng JY, Botte J, Cotrufo MF (2013) Co-generated fast pyrolysis biochar mitigates green-house gas emissions and increases carbon sequestration in temperate soils. *Glob Change Biol Bioenergy* 5(2):153–164. doi:[10.1111/gcbb.12001](https://doi.org/10.1111/gcbb.12001)
- Stocks BJ, Fosberg MA, Lynham TJ, Mearns L, Wotton BM, Yang Q, Jin JZ, Lawrence K, Hartley GR, Mason JA, McKenney DW (1998) Climate change and forest fire potential in Russian and Canadian boreal forests. *Clim Change* 38(1):1–13. doi:[10.1023/a:1005306001055](https://doi.org/10.1023/a:1005306001055)
- Strobel BW, Hansen HCB, Borggaard OK, Andersen MK, Raulund-Rasmussen K (2001) Composition and reactivity of DOC in forest floor soil solutions in relation to tree species and soil type. *Biogeochemistry* 56(1):1–26. doi:[10.1023/a:1011934929379](https://doi.org/10.1023/a:1011934929379)
- Tappi (1981) Water solubility of wood and pulp. Test method T204 (or 207). Technical Association of the Pulp and Paper Industry, Atlanta
- Thomas CD (2010) Climate, climate change and range boundaries. *Divers Distrib* 16(3):488–495. doi:[10.1111/j.1472-4642.2010.00642.x](https://doi.org/10.1111/j.1472-4642.2010.00642.x)
- Van Soest PJ, Wine RH (1968) Determination of lignin and cellulose in acid-detergent fiber with permanganate. *J Assoc Off Anal Chem* 51(4):780
- Van Soest PJ, Robertson JB, Lewis BA (1991) Methods for dietary fiber, neutral detergent fiber, and nonstarch polysaccharides in relation to animal nutrition. *J Dairy Sc* 74(10):3583–3597. doi:[10.3168/jds.S0022-0302\(91\)78551-2](https://doi.org/10.3168/jds.S0022-0302(91)78551-2)
- Wang WJ, Dalal RC, Moody PW, Smith CJ (2003) Relationships of soil respiration to microbial biomass, substrate availability and clay content. *Soil Biol Biochem* 35(2): 273–284. doi:[10.1016/s0038-0717\(02\)00274-2](https://doi.org/10.1016/s0038-0717(02)00274-2)
- White KE, Reeves JB III, Coale FJ (2011) Mid-infrared diffuse reflectance spectroscopy for the rapid analysis of plant root composition. *Geoderma* 167–68:197–203. doi:[10.1016/j.geoderma.2011.08.009](https://doi.org/10.1016/j.geoderma.2011.08.009)